An Experimental Dual Polarization Antenna Feed for Three Radio Relay Bands

By R. W. DAWSON

(Manuscript received April 26, 1956)

The fundamental problems associated with coupled-wave transducers which operate over a 3-to-1 frequency band have been explored and usable solutions found. The experimental models described are directed toward the broad objectives of feeding the horn-reflector antenna with two polarizations of waves in the 4-, 6- and 11-kmc radio relay bands.

INTRODUCTION

There are at least two communications problems which require frequency selective filters that operate in waveguides over an approximately 3-to-1 frequency interval: (1) channel-separation filters for a circular-electric waveguide system in which it is desirable to use the medium from perhaps 35 to 75 kmc,[1] and (2) band-separation networks needed for the horn reflector antenna that permits simultaneous transmission or reception in the 4, 6 and 11 kmc bands with both polarizations.[2, 3] The research reported in this paper was directed at determining the capabilities of coupled-wave transducers for solving such problems. Experimental work was directed toward the second problem (above) because it is more immediate.

Fig. 1, which is a schematic representation of the feed array, comprised of three sets of directional couplers, shows that the 4-kmc bands are

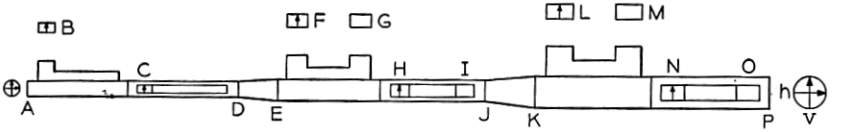

Fig. 1 — Schematic of dual-polarization feed for three microwave bands.

separated one at a time at the antenna end of the array. The 6-kmc bands are separated next and the 11-kmc bands are added or removed at the far end of the array.

GENERAL OBJECTIVES

Negligible loss of power should result when coupling $TE_{10}^{\square}$ waves to $TE_{11}^{\bigcirc}$ waves for the six bands concerned.* The 6- and 11-kmc waves of both polarizations must pass through the round guide of the 4-kmc transducers without significant attenuation. Waves in the 11-kmc band must also pass through the circular guide of the 6-kmc transducers without appreciable loss. A good impedance match is desired at all ports. No cross coupling is desired between the orthogonally polarized waves in the round guide.

FUNDAMENTAL PROBLEMS ENCOUNTERED

The frequency-selectivity required to separate various bands in the same polarization can be achieved in a coupled-wave device by either varying the coupling coefficient and/or varying the phase constant, as illustrated by the expression for the amplitude of the selected wave:[4]

$$|E| = \frac{1}{\sqrt{1 + \left(\frac{\beta_1 - \beta_2}{2c}\right)^2}} \sin\left\{\sqrt{1 + \left(\frac{\beta_1 - \beta_2}{2c}\right)^2}\right\} cx \qquad (1)$$

where c = coupling coefficient

x = length of coupling array

β = phase constant

In the present designs some of the frequency selectivity is in the coupling holes. The greater part of the selectivity is in the design of the phase constants; they are made equal in the band to be selected ($\beta_1 - \beta_2 = 0$) and very unequal

$$\left(\frac{\beta_1 - \beta_2}{2c} \gg 2c\right)$$

in the frequency bands to be passed.

The size of the coupling hole must be controlled to avoid coupling hole resonance in any of the three bands that may be present. This problem is especially bothersome in the 4 kmc coupler where signals are present

* As used in this article, superscripts ○ and □ refer to round and rectangular waveguides, respectively.

in all three bands. To keep the coupler length within a reasonable size, the individual hole dimensions must be on the order of $\lambda_0/4$ (at 4 kmc), which *will* permit coupling hole resonance within the 3-to-1 frequency band. A further consideration is the selection of the hole shape to avoid perturbing the TE_{11}° wave that is orthogonal to the strongly coupled TE_{11}° wave.

Spacing of the coupling holes must *not* be $\lambda_g/2$ to avoid: (1) large reflections in the driven waveguide, and (2) large backward-travelling waves in the adjacent coupled waveguide. This requirement is easily met in the 11-kmc coupler where only one band is present; however, the presence of signals in two or three bands makes the non $\lambda_g/2$ spacing more difficult in the 6- and 4-kmc couplers.

Another phenomena of importance exists in coupled waveguides operating over an extended frequency range. A coupling aperture in the side wall (see Fig. 1) may interact with a high-order mode at the latter's cutoff frequency, resulting in a significant perturbation of the desired coupling. For example, at the frequency where TE_{21}° passes through cut off, the coupling between TE_{11}° and $TE_{10}^{\square}$ will be perturbed *if* the coupling hole is of sufficient size. Small coupling holes do not allow this perturbation to manifest itself. Coupling holes in a realistic design do become large enough to allow this effect to appear. Since dominant mode guides in the 4- and 6-kmc bands can support other modes in the higher frequency bands, considerable caution must be exercised in selecting the round guide sizes on this account alone. (The size of the round guide is determined also by the phase velocity in the rectangular guide).

SELECTION OF COUPLING APERTURES

A series of holes in either the narrow or broad side of the rectangular guide can, in principle, be used to achieve complete power transfer from $TE_{10}^{\square}$ waves to TE_{11}° waves. The specific consequences of coupling through holes located along the center line of the broad side will be considered first. (Off center holes are not of interest because they couple $TE_{10}^{\square}$ waves to both polarizations of TE_{11}° waves in a frequency-sensitive way.) The transverse magnetic field H_φ and the electric field E_ρ of the TE_{11}° waves can couple to $TE_{10}^{\square}$ waves. When two fields couple, the backward wave in the undriven guide can be greater than the forward wave in the same guide. To avoid this possibility, transverse slots can be used to prevent electric field coupling. The coupling of a transverse slot increases as the frequency is increased which suggests that 11 kmc signals be introduced at the position nearest to the antenna because the largest tolerable apertures for an 11-kmc coupler would not perturb 6- or 4-kmc

waves. Unfortunately, coupling to slots in this orientation is small, requiring several hundred for complete power transfer. Such a large number would make the coupler too long.

Coupling through holes in the center of the narrow wall of the rectangular waveguide as shown in Fig. 2 allows only the longitudinal magnetic field H_z to couple when the electric field of the TE_{11}° wave is parallel to the hole containing wall. No coupling exists between the $TE_{10}^{\square}$ waves and the TE_{11}° wave having an electric field perpendicular to the plane of the hole. The use of longitudinal slots where practicable minimizes perturbation of this wave. Since the desired $TE_{10}^{\square} - TE_{11}^{\circ}$ coupling decreases by 15 db from the 4 kmc to the 11 kmc bands (for $1.872 \times 0.872''$ and 2.2″ diam. guide), the layout of Fig. 1 suggests itself since some coupling discrimination is present for the higher frequency waves that pass through the lower frequency couplers.

DESIGN OF 11-KMC COUPLER

The objective of this design is to transfer all of the power from a dominant mode rectangular guide into one polarization of the TE_{11}° forward traveling wave in an adjacent circular guide. Fundamental coupled-wave theory[4] shows that phase velocities must be matched in the two guides to achieve complete power transfer.

A standard rectangular guide size is selected and the round guide size that has the same phase constant is calculated for the center of the 1,000-mc wide band. An approximate total length is selected for the series of coupling holes that permits the holes to be spaced approximately $\lambda_g/4$ apart. The hole spacing is not critical although the nondirectional properties of $\lambda_g/2$ spacing must be avoided. The required magnitude of multiple discrete couplings is shown in equation (40) of Reference 4 to be:

$$\alpha = \sin\left(\frac{\pi/2}{n}\right) \tag{2}$$

where n is the number of coupling holes and α is the amplitude of the wave transferred at a single coupling hole for unit incident amplitude.

Equation (3) expresses the power coupled from TE_{11}° waves to $TE_{10}^{\square}$ waves through a circular hole in a common wall of zero thickness where P_2 is the power propagating away from the coupling point in either direction in the undriven guide, and P_1 is in the driven guide. This derivation is based on the work of H. A. Bethe[5] and some unpublished notes of S. P. Morgan.

$$\frac{P_2}{P_1} = \frac{0.6805\lambda_0^2 r^6}{ba^3R^4\sqrt{1-\left(\frac{\lambda_0}{2a}\right)^2}\sqrt{1-\left(\frac{\lambda_0}{3.413R}\right)^2}} \tag{3}$$

The quantities a and b are the large and small dimensions of the rectangular waveguide and R is the round guide radius. The wavelength in air is designated by λ_0, and the radius of the coupling hole by r. A correction for the finite thickness of the wall is made by considering the circular coupling hole to be a round waveguide beyond cutoff.[6] The additional loss is

$$\Delta = \frac{16t}{r}\sqrt{1-\left(\frac{3.413r}{\lambda_0}\right)^2} \text{ (decibels)} \tag{4}$$

where t is the wall thickness. Total coupling loss per hole is defined by

$$20 \log_{10} \alpha = 10 \log \frac{P_2}{P_1} - \Delta \tag{5}$$

The number of coupling holes n is found from the approximate coupling length and hole spacing. Equation (2) is used to find α and then the hole radius r is calculated from (3).

Waveguide dimensions must be corrected to allow for the perturbation of the phase constants due to the coupling holes. The perturbed phase constant* for the round guide is

$$\beta_p{}^{\circ} = \beta^{\circ} + \frac{\sqrt{p^{\circ}}}{d} \tag{6}$$

where d is the hole spacing and p° is the coupling between a pair of round guides

$$p^{\circ} = \frac{0.1056r^6\lambda_0^2}{R^8\left[1-\left(\frac{\lambda_0}{3.413R}\right)^2\right]} \tag{7}$$

The perturbed phase constant for the rectangular guide is

$$\beta_p{}^{\square} = \beta^{\square} + \frac{\sqrt{p^{\square}}}{d} \tag{8}$$

$$p^{\square} = \frac{4\pi^2 r^6\lambda_0^2}{9a^6b^2\left[1-\left(\frac{\lambda_0}{2a}\right)^2\right]} \tag{9}$$

* This correction is due to S. A. Schelkunoff as noted on page 708 in Reference 4.

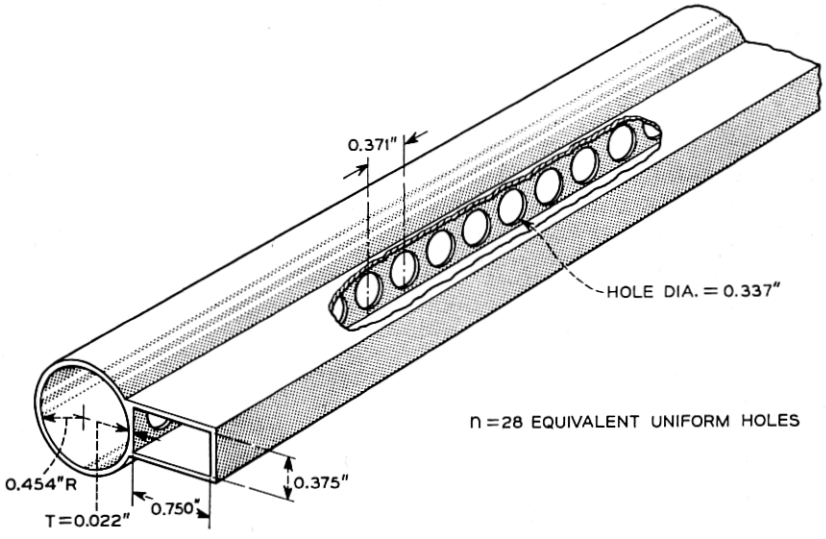

Fig. 2 — 11-kmc coupler sketch.

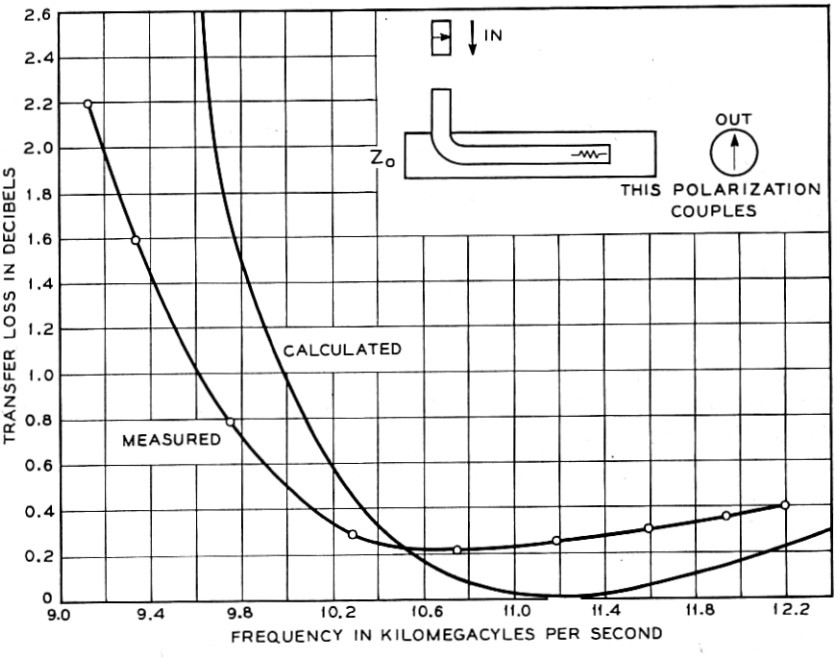

Fig. 3 — 11-kmc coupler transfer loss.

The perturbed phase constants are made equal through a suitable choice of R and a, this choice being somewhat influenced by the coupling-hole radius r.

Three coupling apertures of successively reduced size are used at the ends of the array of identical holes to produce four reflections having the relative amplitudes of 1, 2.7, 2.7, 1. The modified binomial distribution was chosen because impedance matching can be secured over a broader

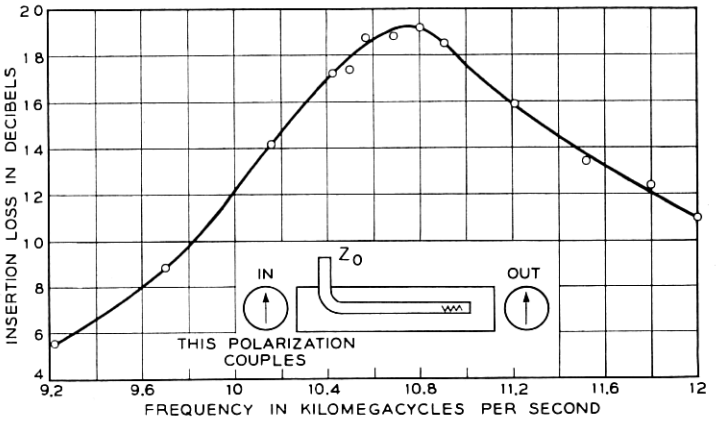

Fig. 4 — 11-kmc coupler insertion loss.

band (with minor degradation of the center-frequency match) when compared to a standard binomial distribution. Amplitude reflections* from the start of the coupling array are

$$A_r = \frac{\lambda_g Q}{4\pi d} \tag{10}$$

where Q is the reflection from a single coupling hole.

Fig. 2 is a sketch of the coupler with the final design dimensions. Fig. 3 shows the measured and theoretical transfer loss of an 11 kmc coupler. Fig. 4 indicates the measured insertion loss for the same coupler.

DESIGN OF 6-KMC COUPLER

The 6-kmc coupler as shown in Fig. 5 utilizes a partially dielectric-filled rectangular guide coupled to the circular guide. The use of dielectric loading makes it possible for the phase velocities to be equal in the two guides in the center of the 500-mc wide 6-kmc band, and unequal in

* Information given to S. E. Miller by S. A. Schelkunoff in an informal communication.

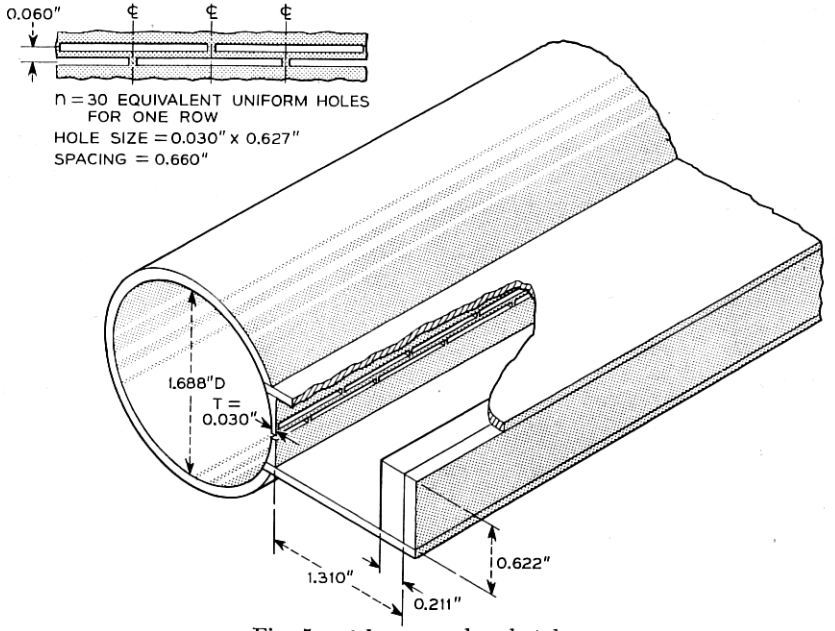

Fig. 5 — 6-kmc coupler sketch.

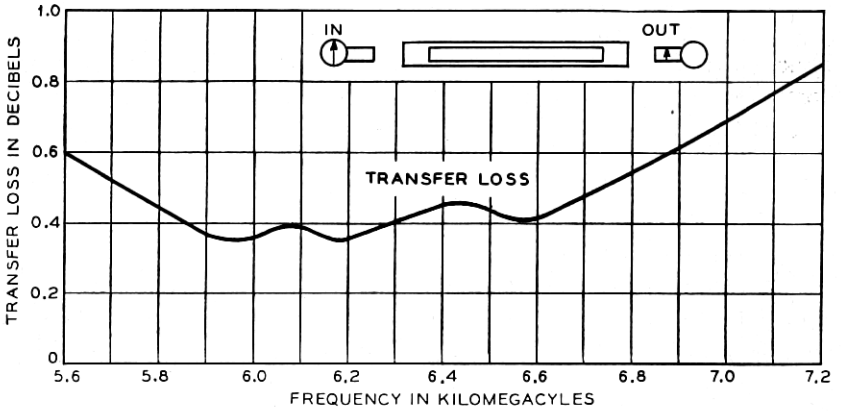

Fig. 6 — Transfer loss of 6-kmc coupler.

the 11-kmc band; thereby low transfer loss is obtained in the 6-kmc band and a high transfer loss in the 11-kmc band. Measurements have shown that when the cut-off frequencies of higher modes occur in the band of interest an uncontrolled increase of coupling may result. Special precautions are required in selecting the round guide size to avoid this condition. The design process is shown in Appendix I. Figs. 6 and 7 show the transfer and insertion losses in the 6-kmc band.

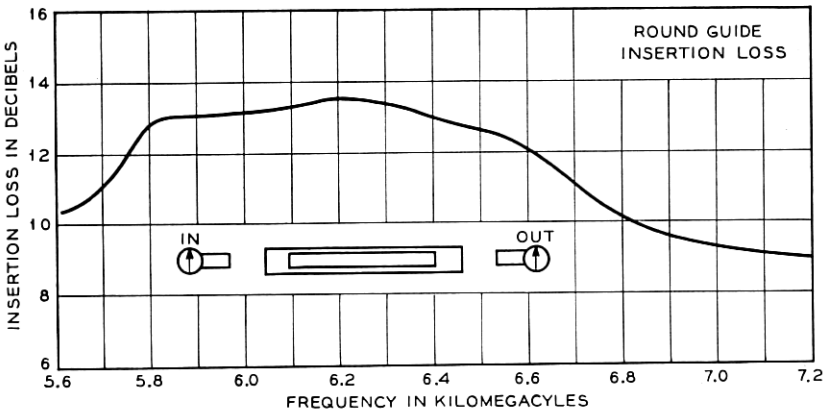

Fig. 7 — Insertion loss of 6-kmc coupler.

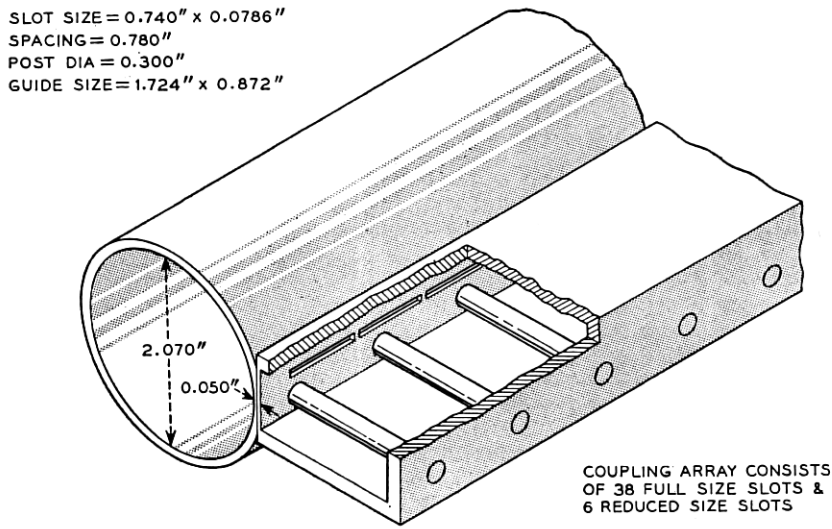

Fig. 8 — 4-kmc coupler sketch.

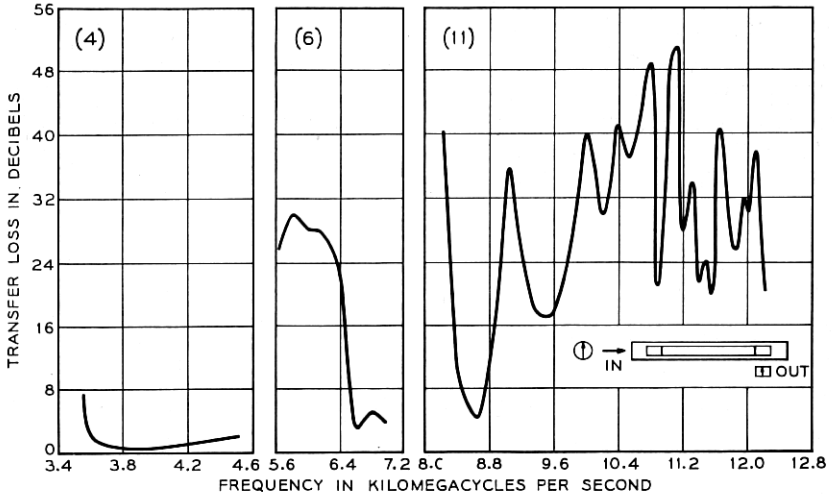

Fig. 9 — Transfer loss of 4-kmc coupler in 4-, 6- and 11-kmc bands.

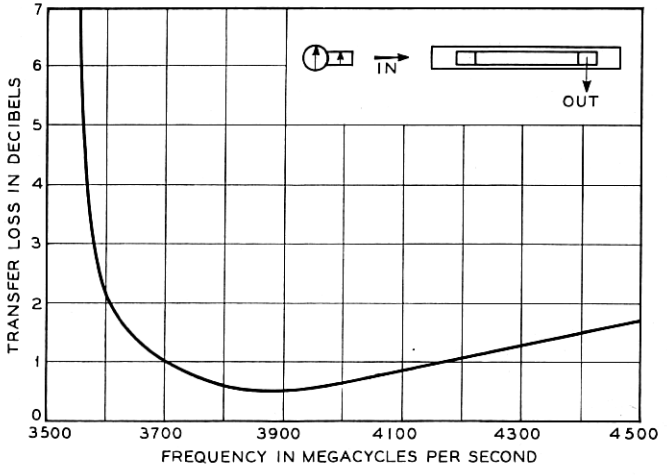

Fig. 10 — Transfer loss of 4-kmc coupler in 4-kmc band.

4-KMC DESIGN

The use of periodic loading in the rectangular guide is not suitable for use in a 4-kmc coupler design. When the phase constants are made equal in the 4-kmc band, the resulting difference of phase constants in the 6-kmc band is too small to create a sufficiently high transfer loss in that band. Periodic loading can produce the desired result.

Capacitive rods form a periodic structure in the rectangular guide, as shown in Fig. 8, that creates a rejection band in the 6-kmc region. Fig. 9 illustrates how effectively the rejection band increases the transfer loss in the 6-kmc region. Phase velocities are made equal in the rectangular and round guides at the center of the 500-mc wide 4-kmc band to secure a low transfer loss. Due to the rejection bands and the difference of phase constants, high transfer losses result in the 6- and 11-kmc bands. To prevent uncontrolled coupling the round guide size is chosen so that no modes cut off in the three bands. Details of the design are covered in Appendix II. Figs. 10 and 11 show the measured transfer and insertion losses in the 4-kmc band.

MEASURED CHARACTERISTICS OF ARRAY

The three pairs of couplers were assembled in a tandem array with linear taper sections between them. In the discussions that follow the port designations of Fig. 1 will be used. Transfer loss measurements indicate

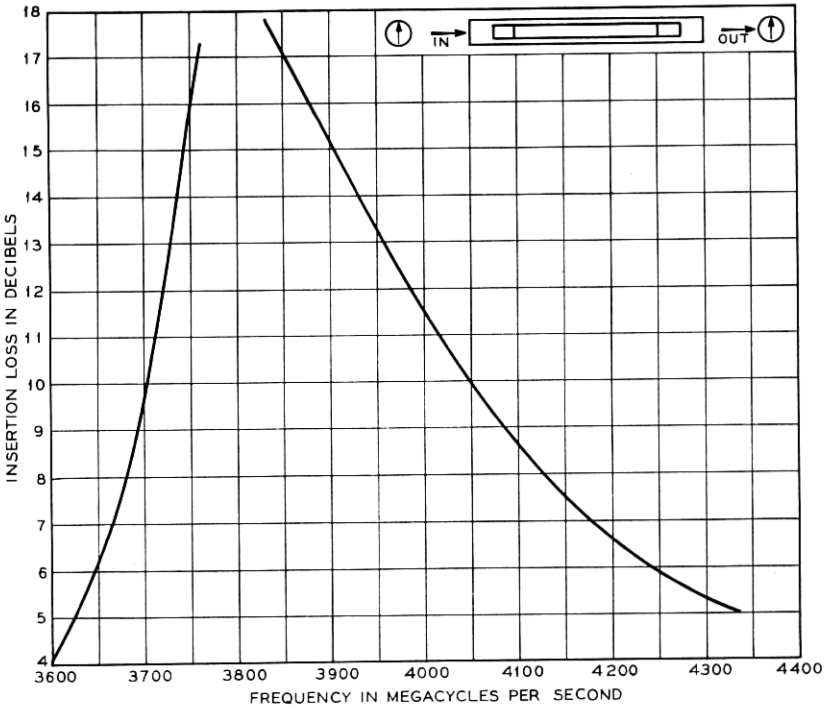

Fig. 11 — Insertion loss of 4-kmc coupler in 4-kmc band.

how much power in a forward traveling TE_{11}° wave is transferred to a forward traveling $TE_{10}^{\square}$ wave. Figure 12 shows that the coupling polarization transfer loss remains under 1.1 db in the three bands except for a small region in the 11-kmc band, while the transfer loss for the non-coupling polarization exceeds 20 db in the three regions as shown in Fig. 13. The return loss at Port P exceeded 23 db over the 4-kmc band. This result included the total reflection of 4-kmc signals from Taper *J-K* after attenuation by twice the coupler insertion loss, and also included the reflections from the rectangular guide port *N* or *L* which

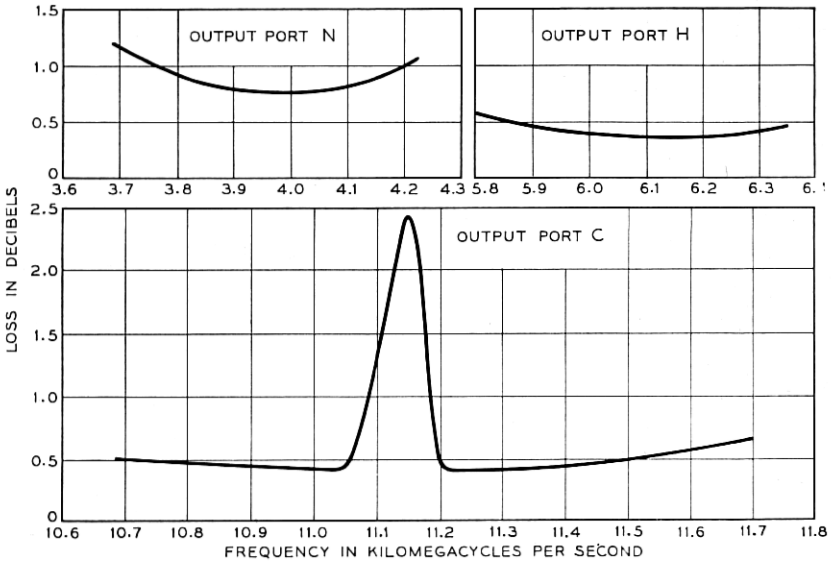

Fig. 12 — Transfer losses in the array for coupling polarization.

are separated from *P* by only the small transfer loss. Return loss for the 6- and 11-kmc bands exceeded 23 db at Port *P*. Cross polarization is the ratio of the energy in the coupling polarization waves to the orthogonal non-coupling polarization waves emerging at Port *P*. Cross polarization figures are no lower than 20, 32 and 22 db in the 4,-6- and 11-kmc bands.

CONSTRUCTION OF COUPLERS

The coupler design requires that the coupling aperture exist in a narrow wall of the rectangular guide that is common to the round guide. The 4-kmc coupler consists of machined rectangular and round sections. A two-piece rectangular guide was milled from brass and

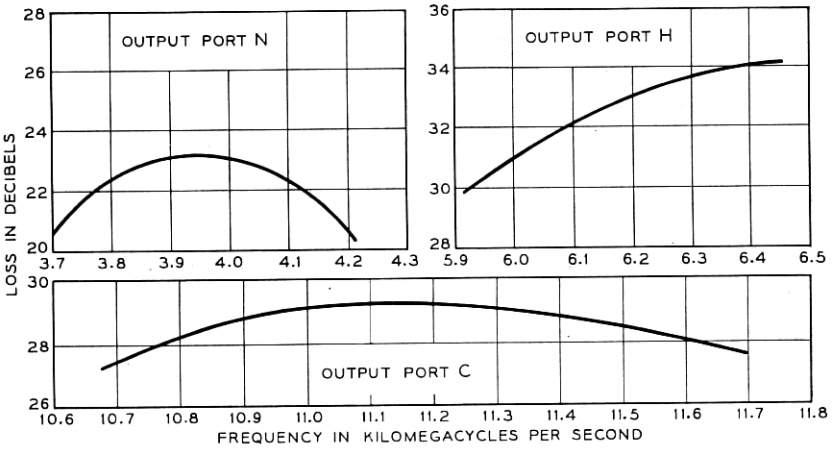

Fig. 13 — Transfer losses in the array for non-coupling polarization.

soldered to the round guide. The coupling slots were then cut through the common wall. An electroforming technique was used to fabricate the 6- and 11-kmc couplers. A rectangular guide with precut coupling holes was clamped to a round mandrel and the entire structure was electroformed. The mandrel was later removed by dissolving it in a hot concentrated solution of sodium hydroxide. A typical mandrel and rectangular guide is shown in Fig. 14. An illustration of the entire ensemble appears as Fig. 15.

DESIGN REFINEMENTS

Return loss at the round Port P might be improved in a revised design by broad-banding the $TE_{10}^{\square}$-$TE_{11}^{\bigcirc}$ transfer loss, with an associated increase in the $TE_{11}^{\bigcirc}$ insertion loss. This might be done without introducing mode troubles, by using ridged waveguide. In Fig. 12 the abrupt peak of transfer loss for coupling polarization waves in the 11

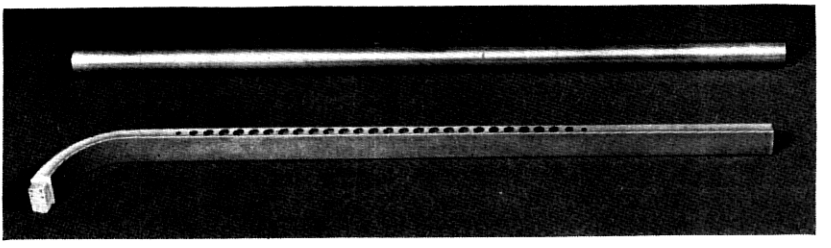

Fig. 14 — Mandrel and rectangular guide.

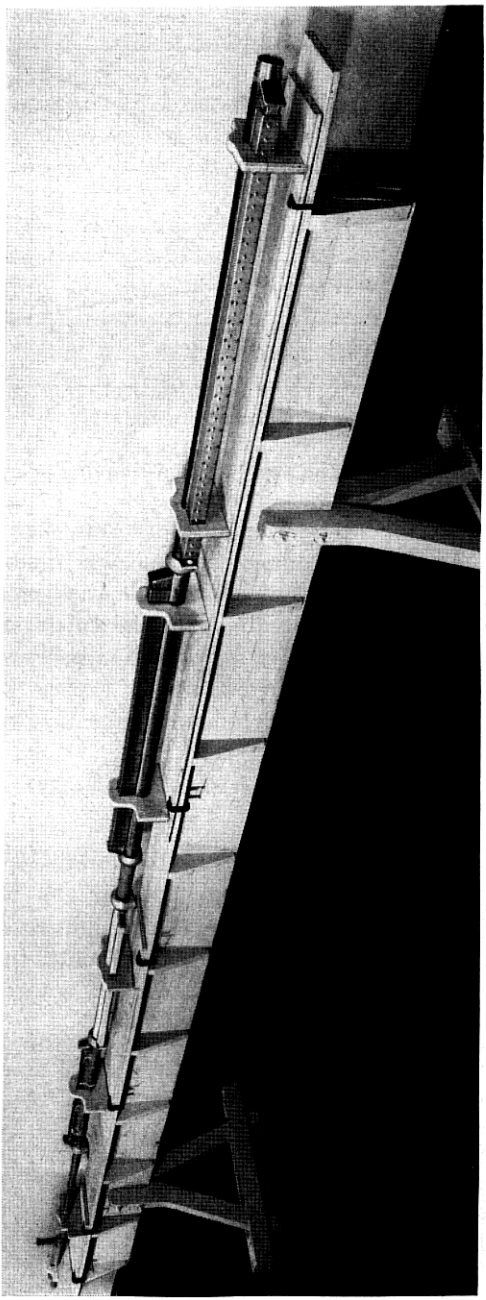

Fig. 15 — The array.

kmc band is due to an appreciable coupling of TE_{11}° waves to $TE_{30}^{\square}$ waves in the 4 kmc couplers in the vicinity of the $TE_{30}^{\square}$ cutoff. The $TE_{30}^{\square}$ cutoff might be moved above the 11-kmc band by using ridged rectangular guide.

SUMMARY

A combination of three pairs of coupled-wave transducers has successfully permitted six distinct bands to be fed from individual $TE_{10}^{\square}$ rectangular waveguides into the two orthogonal polarizations of TE_{11}° waves in a multi-mode round waveguide. The resulting structure enabled low transfer loss values to be obtained simultaneously over two 500-mc wide bands and one band 1000-mc wide distributed over a 3-to-1 frequency interval.

ACKNOWLEDGMENT

A substantial portion of this work was carried out as a joint project with H. E. Heskett and S. E. Miller.

Appendix I

DESIGN OF 6-KMC COUPLER

A rectangular guide size is chosen and a reasonable value selected for the phase constant such as $\beta^{\square} = 1.5\pi/\lambda_0$. The resulting round guide size must prevent modes from cutting-off within the 6-kmc band and preferably the cut-off frequency should be above the 6-kmc band. The thickness of the dielectric (polystyrene) strip is determined[7] from (11), (12), and (13) where K_1 and K_2 are transverse wave numbers of the air-filled and of the dielectric sections of the guide.

$$K_1 = \sqrt{\left(\frac{2\pi}{\lambda_0}\right)^2 - \beta_{\square}^2} \tag{11}$$

$$K_2 = \sqrt{\varepsilon_r \left(\frac{2\pi}{\lambda_0}\right)^2 - \beta_{\square}^2} \tag{12}$$

$$\text{Cot } K_2 d = -\frac{K_1}{K_2} \cot K_1(a - d) \tag{13}$$

In the above equations ε_r is the relative dielectric constant and d is the slab thickness. After solving for d the equations are resolved for K_1 and K_2 values at the 6-kmc band edges and also at the lower end of the 11-kmc band. Resulting rectangular-guide phase constants should cause a very

low and a high value of transfer loss as indicated by (14) which represents the forward traveling coupled wave amplitude where cx is the total coupling strength.[4]

$$E_2 = \frac{1}{\sqrt{\frac{(\beta_\square - \beta_\bigcirc)^2}{4c^2} + 1}} i \sin\left[\sqrt{\frac{(\beta_\square - \beta_\bigcirc)^2}{4c^2} + 1}\right] cx \tag{14}$$

At midband $cx = \pi/2$ and experience has shown $x \cong 10\ \lambda_0$; therefore $c \cong \pi/20\lambda_0$ at midband. The coupling hole radius is found from (3). Because longitudinal slots are used instead of round holes the equivalent hole radius r is found from $\frac{4}{3}r^3 = P\ell^3$, where P is the magnetic polarizability[8] and ℓ is the length of the chosen slot. To avoid slot resonance in either band, the length was chosen to be approximately $\lambda_0/4$ in the 6-kmc band and $\frac{5}{8}\lambda_0$ in the 11-kmc band. The power expression of (3) must be corrected by the wall thickness effect (4) and also multiplied by the factor F due to the presence of the dielectric slab[7] (15).

$$\begin{aligned} F &= \frac{2a^3K_1^4}{\pi\beta_\square\lambda_\square[K_1(\theta_1 - \tfrac{1}{2}\sin 2\theta_1) + A^2K_2(\theta_2 - \tfrac{1}{2}\sin 2\theta_2)]} \\ \theta_1 &= K_1(a - d) \qquad \theta_2 = k_2 d \qquad A = \left(\frac{K_1}{K_2}\right)^2 \frac{\cos\theta_1}{\cos\theta_2} \end{aligned} \tag{15}$$

Theoretical coupling loss per hole is defined by

$$20 \log_{10} \alpha = 10 \log \frac{P_2}{P_1} - (\Delta + 10 \log_{10} F) \tag{16}$$

An additional correction which reduces the coupling loss is due to the long length of the slot. Although the slot resonates near 9 kmc, an increase of 3 db in a single slot coupling results at 6 kmc. This effect was found experimentally from a sample test line with several slots. To avoid excessive length two rows of coupling slots were employed. They were staggered to improve the continuity of coupling from discrete points. An approximate design is on hand at this point. The final dimensions for the guides and coupling holes are found after the perturbations of the phase constants are considered by the same process as noted in the discussion of the 11-kmc design. Impedance matching for the dielectric strip and the coupling slot array was patterned after the technique shown for the coupling hole array in the 11 kmc design.

Appendix II

DESIGN OF 4-KMC COUPLER

A round guide size is selected so that no modes are cut-off in the three bands. Coupling power varies with wavelength as shown in (17) for TE_{10} to $TE_{11}{}^{\circ}$ coupling.

$$Y = \frac{\lambda_0^2}{\left[1 - \left(\frac{\lambda_0}{3.413R}\right)^2\right]} \tag{17}$$

To maintain the minimum variation across the band, the following requirements must be met which were deduced from the coupled wave theory[4] and (17).

$$\sin (cx)_1 = \sin (cx)_2 \tag{18}$$

$$\frac{(cx)_1}{(cx)_2} = \frac{\lambda_0}{\sqrt{1 - \left(\frac{\lambda_0}{3.413R}\right)^2}} \tag{19}$$

$$(cx)_1 + (cx)_2 = \pi \tag{20}$$

The equations are solved for sin cx (the minimum band edge transfer loss) which for a diameter of 2.10″ is 0.5 db. A value of 30 db is chosen for α, (2), as the first approximation. Because the band edge transfer loss is 0.5 db due to frequency variation of coupling, an additional loss of only 0.2 db is allowed for the phase constant difference $(\beta_L{}^{\square} - \beta^{\circ})$. It is now necessary to make $\beta^{\circ} = \beta_L{}^{\square}$, where $\beta_L{}^{\square}$ is the phase constant of the loaded rectangular guide. Equation (21) gives a theoretical periodic loading formula where L is the spacing between loading elements.[9]

$$\cos \beta_L{}^{\square} L = A \cos (\beta^{\square} L + \Phi)$$
$$\Phi = \arctan \frac{b_0}{2} \quad A = \sqrt{1 + \left(\frac{b_0}{2}\right)^2} \tag{21}$$

Assume initially that $L = \pi/\beta^{\circ}$. The required susceptance b_0 of the capacitive rods can be found experimentally from a loaded test line by varying b_0 until the first rejection band covers the 6 kmc band. An iterated process is used to find L because it is dependent on $\beta^{\square}$ which is the parameter being sought. Measurements indicated that (21) does not predict $\beta^{\square}$ very accurately and for that reason an experimental adjustment of $(\beta_L{}^{\square} - \beta^{\circ})$ is desirable.

The guide dimensions are now known; however, they must be corrected for the perturbations of the phase velocities as outlined in the 11-

kmc coupler design. A single row of longitudinal coupling slots which are not resonant in the 6- or 11-kmc bands is used. The radius of a round hole equivalent to the slot is obtained as in Appendix I, by setting $\frac{4}{3}r^3 = P\ell^3$.

Impedance matching of the coupling array and of the loading elements is accomplished by tapering the amplitude of the end elements as indicated by a discrimination function of the coupled wave theory.[4] For a 5 element series $1 - n_1 - n_2 - n_1 - 1$

$$D = \frac{2(n_1 + 1) + n_2}{2\left(n_1 \cos \frac{4\pi Z}{\lambda_g} + \cos \frac{8\pi Z}{\lambda_g}\right) + n_2} \tag{22}$$

where Z is the spacing between elements.

The discrimination D is set equal to infinity which permits the denominator to be set equal to zero and solved simultaneously for n_1 and n_2 by using both band edge wave-lengths. Round hole sizes are readily obtained since the coupling coefficient is directly proportional to the cube of the hole radius from which the necessary equivalent longitudinal slot can be calculated. Susceptance values of the capacitive posts are found from the absolute value of the reflection coefficient which equals

$$\frac{b_0}{\sqrt{b_0^2 + 4}}$$

REFERENCES

1. S. E. Miller, Waveguide as a Communication Medium, B.S.T.J., Nov., 1954.
2. A. T. Corbin and A. S. May, Broadband Horn Reflector Antenna, Bell Laboratories Record, **33,** p. 401, Nov., 1955.
3. A. P. King, Dominant Wave Transmission Characteristics of a Multimode Round Waveguide, Proc. I.R.E., **40,** Aug., 1952.
4. S. E. Miller, Coupled Wave Theory and Waveguide Applications, B.S.T.J., May, 1954. (See page 681.)
5. H. A. Bethe, Physical Review, **66,** p. 63, 1944. Also Report 43-22, Lumped Constants for Small Irises, Mar. 24, 1943; Report 43-26, Formal Theory of Wave Guides of Arbitrary Cross Section, Mar. 16, 1943; and Report 43-27, Theory of Side Windows in Wave Guides, Apr. 4, 1943; from M.I.T. Radiation Lab.
6. N. Marcuvitz, Waveguide Handbook, p. 408, McGraw Hill.
7. H. Seidel, private communication re: Slab Width Determination and Effects on Coupling Parameters in Partial Dielectric Loading.
8. S. B. Cohn, Determination of Aperture Parameters by Electrolytic Tank Measurements, Proc. I.R.E., Nov., 1951.
9. J. C. Slater, Microwave Electronics, p. 183, Van Nostrand.